We are IntechOpen, the world's leading publisher of Open Access books Built by scientists, for scientists

6,400
Open access books available

174,000
International authors and editors

190M
Downloads

154
Countries delivered to

Our authors are among the

TOP 1%
most cited scientists

12.2%
Contributors from top 500 universities

CLARIVATE ANALYTICS
BOOK CITATION INDEX
INDEXED

WEB OF SCIENCE™

Selection of our books indexed in the Book Citation Index
in Web of Science™ Core Collection (BKCI)

Interested in publishing with us?
Contact book.department@intechopen.com

Toward an Instrumented Strength Microprobe – Origins of the Oliver-Pharr Method and Continued Advancements in Nanoindentation: Part 1

Bryer C. Sousa, Jennifer Hay and Danielle L. Cote

Abstract

Sub-micron instrumented indentation testing and standardized nanoindentation testing systems have become commonplace within the materials engineering community. Though commonly utilized for mechanical characterization, general appreciation and understanding of the governing theory, formulations and best practices underpinning modern nanoindentation systems appears to remain relatively elusive to the general materials science and engineering community as well as nanoindentation practitioners using such systems for mechanical assessment. Accordingly, the present chapter details how nanoindentation methods emerged and how the Oliver-Pharr method of nanoindentation testing and analysis was constructed and refined to yield theoretically consistent and readily implementable attributes for probing small-scale mechanical properties via microscopy free indentation testing.

Keywords: nanoindentation, depth-sensing indentation testing, instrumented indentation testing, Oliver-Pharr method, hardness, modulus, load-displacement

1. Introduction

Motivated by the need for a consistent and implementable method for performing sub-micron instrumented indentation tests (IIT) on materials, as well as for analyzing IIT data at the micro- and nanometer scales, Oliver and Pharr (O&P) improved upon the work of Doerner and Nix (D&N) and others in Ref. [1]. They focused on the work of D&N [2] because they found that D&N's assumption of linearity in the upper one-third of the indentation load-displacement curve was inconsistent with O&P's observations across various materials subject to small-scale IIT. Prior to the publication of O&P's findings in 1992, the Doerner-Nix (DN) method was considered the most comprehensive approach for determining hardness (H) and elastic modulus (E), but it was replaced by the Oliver-Pharr (OP) method after publication.

Motivated by the need for a theoretically consistent and practically implementable modality of performing sub-micron or small volume instrumented indentation testing (IIT) of materials, as well as the need for a method of analyzing IIT test data at the micrometer and nanometer length scales, Oliver and Pharr (O&P) refined and considered the foundational work of Doerner and Nix (D&N), among others, in Ref. [1]. O&P gave particular attention to the work of D&N [2] due to O&P's discovery that D&N's assumed linearity of the upper one-third of a given indentation load-displacement unloading curve was at odds with O&P's regular experimental observations across numerable material types. Until O&P published their findings in 1992, the Doerner-Nix (DN) method for determining both hardness (*H*) and modulus of elasticity (*E*), or Young's modulus, was thought to be the most thorough load-displacement data analysis approach prior to the introduction of the Oliver-Pharr (OP) method of testing and analysis.

With such significance and implications in mind, O&P set out to address standing issues, problems, and inadequacies associated with the DN method of sub-micron indentation testing and data analysis. Beyond simply demonstrating that unloading curves are rarely, if at all, linear, O&P went on to substantiate their hypothesis that unloading curves ought to be thought of as nonlinear and power-law-based. O&P presented load-displacement data for an array of materials (ranging from crystalline ceramics to amorphous glasses as well as both soft and hard cubic-centered metals) to demonstrate said non-linearity of unloading data [1].

In addition to the presentation of such substantiating nanoindentation load (*P*) vs. displacement or depth (*h*) data, data analysis, and resultant findings, the OP method was carefully documented such that physically justifiable indentation depth determination was reliably and repeatably procurable. Furthermore, the resultant abilities brought about by the OP method were further detailed for subsequent use in establishing peak applied load contact areas and contact area functions for various indenter tips and tip geometries. The OP method also provided beneficiaries of nanoindentation testing with a measurement and analysis heuristic for depth determination with load-controlled nanoindentation testing and load-controlled nanoindentation-derived data analysis. Remarkably, O&P had done so while avoiding the use of (or need for) post-indentation microscopy, which not only remains both time-consuming and costly for nanometric resolutions but was also generally out of the reach for many researchers and engineers during the early 1990s.

Upon rendering such findings, *H* and *E* values were then deduced via load-displacement data, as analyzed according to said OP methodology, and then compared with values derived from alternative and independent means to demonstrate the accuracy of the OP method [1]. A discussion was also presented in 1992, which pragmatically coupled theory and practice together, such that load frame compliance and indenter shape functions could be integrated into nanoindentation load-displacement data analysis platforms and experimental nanoindentation frameworks generally.

2. Consideration of the Oliver-Pharr approach

In analytical terms, *h* represents the total nanoindenter displacement, defined mathematically in Eq. (1), such that

$$h = h_c + h_s \tag{1}$$

wherein h_c is the contact depth, or the distance under which indenter tip contact is made normal to the sample surface, and h_s represents the surface displacement (which is now classified in the literature as pile-up, sink-in, or both, depending upon the material deformation mechanics, among other factors) about the contact perimeter. In addition to h, h_c, and h_s, P_{max} captures the load applied during nanoindentation testing at h_{max}, or the maximal IIT displacement achieved during a given test. At the same time, O&P concurrently considered S, a, and h_f too, such that S_{max} was defined as the experimentally measured stiffness (S) obtained via the slope of the tangent line procured from the initial unloading point along the curve, which occurs upon reaching P_{max} at h_{max}.

That said, h_f was defined as the depth of the residual IIT or nanoindentation impression upon both complete unloading and total indenter removal from the specimen, whereas a was presented as a surrogate geometrical contact radius. Considering the discussion presented thus far, **Figure 1(a)** presents load-displacement data at various points along loading and unloading curves. In addition, **Figure 1(a)** also captures their relation to the inelastic work and the work of elastic deformation associated with a given indentation test. Finally, **Figure 1(b)** also presents a cross-sectional view of indentation phenomena.

In addition to Eq. (1), the OP method determines E as expressed in Eq. (2), such that

$$\frac{1}{E_r} = \frac{1 - v^2}{E} + \frac{1 - v^2}{E_i} \tag{2}$$

wherein E_r is the reduced modulus, v is the Poisson's ratio of the specimen, v_i is the Poisson's ratio of the indenter tip, and E_i is the modulus of elasticity associated with the indenter tip material too. Since v_i and E_i are known apriori (let us assume diamond as Eq. (2) is recast for simplicity and consistency with the conventional material utilized as nanoindenter tips), E_r can be solved via another relation and after that substituted back into Eq. (2) such that E can be obtained through
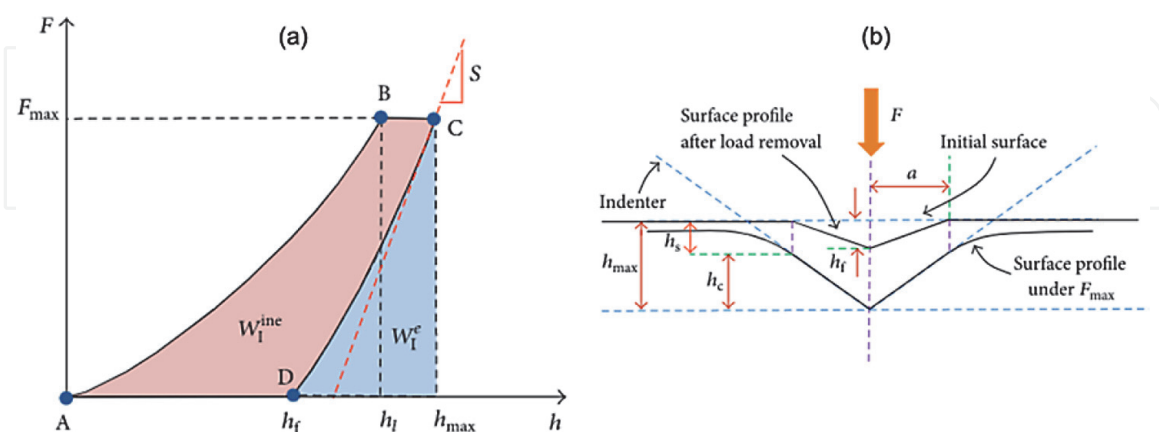

Figure 1.
In (a), A is the initial contact of the indenter tip with the tested material; point B is the point at which the P_{max} is reached; C is the point at which unloading from P_{max} begins after P_{max} is held for a predefined time to account for the influence of creep; D captures h_f, which is reached upon complete unloading; W_I^{ine} is the inelastic work of indentation; W_I^e is the elastic work of indentation; h_l represents the depth associated with B ($h_l = h_{max}$ when creep is not accounted for); S is the experimentally measured stiffness obtained via the slope of the tangent line procured from the load-displacement nanoindentation curve. (b) Presents a cross-sectional view of indentation testing related phenomena (loading and unloading, etc.). Both (a) and (b) were sourced from Ref. [3].

algebraic manipulation and arithmetic. For commonly used diamond indenter tips, we may re-render Eq. (2) to yield Eq. (3):

$$\frac{1}{E_r} = \frac{1 - v^2}{E} + \frac{1 - v^2}{E_i}$$

$$\implies \frac{1 - v^2}{E} = \frac{1}{E_r} - \frac{1 - v_i^2}{E_i}$$

$$\therefore E = \left(1 - v^2\right)\left(\frac{1}{E_r} - \frac{1 - v_i^2}{E_i}\right)^{-1}$$

$$\therefore E = \left(1 - v^2\right)\left(\frac{1}{E_r} - \frac{1 - (0.07)^2}{1140 \text{ GPa}}\right)^{-1}$$

$$\therefore E = \left(1 - v^2\right)\left(\frac{1}{E_r} - \frac{1 - 0.9951}{1140 \text{ GPa}}\right)^{-1} \tag{3}$$

Thus, with knowledge of the test specimen's v and an empirical means of identifying the E_r from load-depth data collection and analysis, E may be readily attained for a given material. That said, Bulychev et al. [4], and others, according to Poon et al. [5], recognized the following relationship between P, h, S, E_r and the projected area of elastic contact (which had been refined and eventually referenced as the contact area per the OP method), expressed as A in Eq. (4), such that

$$S = \frac{dP}{dh}$$

$$= \frac{2E_r\sqrt{A}}{\sqrt{\pi}} \tag{4}$$

Consequently, solving for E_r yields Eq. (5), wherein

$$E_r = \frac{S\sqrt{\pi}}{2\sqrt{A}} \tag{5}$$

and Eq. (5) may therefore be substituted into the previously documented expression for E, which was given in Eq. (2), such that Eq. (6) yields

$$E = 1 - \frac{v^2}{\left(\frac{S\sqrt{\pi}}{2\sqrt{A}}\right)^{-1} - \frac{1 - v_i^2}{E_i}} \tag{6}$$

The mathematical manipulation of said equivalence relations serve as a means of enabling O&P's pedogeological improvements, methodology, and approach to be more explicitly considered. Returning to the matter of fitting loading or unloading segments of load-displacement or load-depth curves via raw nanoindentation data, note that O&P extensively relied upon, as well as critically considered, Sneddon's relation between load and depth for basic punch geometries [6], as presented herein through Eq. (7), wherein

$$P = \alpha h^m \tag{7}$$

In Eq. (7), α, as well as m, are both constants whose values depend on tip geometry. In the case of a flat cylindrical punch geometry, $m = 1.0$. However, in the

case of a conical punch geometry, $m = 2.0$. Additionally, $m = 1.5$ for both spheres at shallow indentation depths and paraboloids of revolution too. One ought to note that Eq. (7) is explicitly related to the loading portion of the complete loading and unloading nanoindentation cycle. Beyond simply revisiting the matter of loading curves, one may also note that the mathematical expression H, which was passively noted above as a discernible mechanical performance indicator (rather than an actual material property [7]) for a given material, may be rendered as Eq. (8), wherein

$$H = \frac{P_{h_x}}{A}$$

(8)

Importantly, O&P also assumed that a given indenter tip geometry might be expressed in terms of an area function, $F(h)$, that relates h with the cross-sectional area of a respective tip. O&P continued their presentation of $F(h)$ through the lens of h_c, given the practical importance of h_c in nanoindentation testing and data analysis, rather than area relations associated with the distance away from the apex of a probe, or h, such that Eq. (9) may be formulated as

$$A = F(h_c)$$

(9)

It is also important to note that O&P regularly reiterated the mathematically expressed rendition of $F(h_c)$, given in Eq. (9), must be determined using the contact area function calibration approach detailed in Ref. [1] before pursuing the application (or use) of the OP data analysis method. Thus, recall that in Eq. (9), $F(h_c)$ functionally relied upon h_c as a means of assessing A. Hence, one ought to observe the fact that h_c can be expressed as a function of h_{max} and h_s, such that Eq. (10) can be presented as

$$h_c = h_{max} - h_s$$

(10)

and thus, pairs well with Eq. (1) too. Nevertheless, the means of ascertaining h_s was noted as being remarkably dependent upon the exact nanoindenter tip geometry utilized. Assuming conical geometries, O&P invoked another expression presented by Sneddon in the 1960s, such that Eq. (11) yields

$$h_s = \frac{\pi - 2}{\pi}(h - h_f)$$

(11)

By way of once again considering one of O&P's intellectual precursors, Ian N. Sneddon of the Department of Mathematics of the University of Glasgow in Scotland, O&P remedied the use of the quantity $(h - h_f)$ in Eq. (11) by way of also invoking Sneddon's load-depth equivalence relation for conical tip geometries, which may be given as Eq. (12), wherein

$$(h - h_f) = \frac{2P}{S}$$

(12)

While it may not seem readily evident as to why Eq. (11) must have been presented in terms of the quantity $(h - h_f)$, rather than h alone, recall the fact that Sneddon's solutions only hold for elastic indentation displacement, rather than the total (i.e., both plastic and elastic portions of indentation deformation phenomena) displacement, which are of course convoluted with one another in unprocessed and experimentally recorded displacement data from a nanoindenter. Thus, the clever

use of Eq. (12) enabled substitutional elimination of the respective $(h - h_f)$ quantity altogether. As a result of the substitution of Eq. (12) into Eq. (11), Eq. (13) can be expressed as follows

$$
\begin{aligned}
h_s &= \frac{\pi - 2}{\pi}(h - h_f) \\
&= \frac{\pi - 2}{\pi}\left(\frac{2P}{S}\right) \\
&= \frac{\epsilon P}{S}
\end{aligned}
\tag{13}
$$

Therefore, when evaluated at P_{max}, Eq. (13) may be rewritten as Eq. (14), where

$$
h_s|_{P=P_{max}} = \epsilon \frac{P_{max}}{S}
\tag{14}
$$

Though ϵ was substituted into Eq. (13) above in place of $2\pi^{-1}(\pi - 2)$, ϵ is variable across tip geometries in a comparable manner to that of m in the case of Eq. (7). Thus, one ought to note that in the case of a flat cylindrical punch geometry, $\epsilon = 1$. However, in the case of a conical punch geometry, $\epsilon = 0.72$. Additionally, $\epsilon = 0.75$ for both spheres at shallow indentation depths and paraboloids of revolution. Also noted earlier was the fact that O&P harped upon the misappropriated assumption of initial unloading load-depth curve linearity by D&N. Alongside such remarks concerned with said critical commentary by O&P, the pair of researchers put forth their simple power-law unloading relation in 1992, as shown in Eq. (15) herein, such that

$$
P = Q\left(h - h_f\right)^k
\tag{15}
$$

wherein all but P and h are determined via applying a least-squares fitting procedure. For comparison with the linear fitting procedure associated with the precursory D&N method of S quantification from sub-micron IIT, O&P presented an underappreciated graphical figure plotted within [1], wherein O&P presented the unloading stiffness obtained for a tungsten specimen as a function of the fraction of the unloading curve considered during data analysis and as a function of using either the DN or OP stiffness determination method applied. Said graphical rendering of peak load stiffness values determined using linear fitting approaches compared to O&P's power law fitting method, coupled with O&P's presentation of the constant stiffness values as a function of the unloading curve considered during data fitting attests to the methodological enhancements and integrity underpinning data interpretation by O&P [1].

In any case, a load frame compliance determination procedure is the next aspect of the OP method to be contextualized and considered herein. For those unfamiliar with the peculiarities of nanoindentation (and load-controlled nanoindenter systems as well as their assembly as a class of scientific instrumentation), the load frame compliance, let alone the importance of such a value, stems from the instrumented method, or modality, incorporated for displacement sensing capabilities via load-controlled systems. More to the point, when an automated and OP compatible IIT characterization suite or nanoindenter is utilized, the raw displacement information recorded by the system must be considered and corrected for both the load frame and the specimen being tested. In turn, precise knowledge of the load frame compliance term enables the unprocessed displacement data

recorded by the system controller to be deconvoluted, algebraically speaking (rather than statistically speaking), such that the displacement contribution from specimen deformation via indentation loading and the displacement contribution from the load frame can be isolated from one another. Consequently, specimen displacements eventually yield indentation depths associated with their respectively applied loads.

However, the mathematics underpinning said displacement deconvolution and analysis, or displacement contribution decoupling, begins with two basic assumptions. The first assumption is that E values are depth-independent, whereas the second assumption is that one may treat said dual compliance terms as a pair of springs in a series, such that Eq. (16) yields

$$C = C_s + C_f \tag{16}$$

wherein C is the measured compliance, C_s is the specimen compliance and C_f is the load frame compliance term. Within the realm of contact mechanics and a given materials' elastic and plastic deformation mechanisms, contact stiffness may be expressed as the inverse of compliance, and compliance may therefore be expressed as the inverse of stiffness. By way of such definitions, in conjunction with Eq. (4) and the spring series-inspired and assumed relation, the substitution of S^{-1} in place of C_s yields Eq. (17), wherein

$$S = \frac{2E_r\sqrt{A}}{\sqrt{\pi}}$$

$$\rightarrow C_s = S^{-1}$$

$$S^{-1} = \frac{1}{S}$$

$$= \frac{\sqrt{\pi}}{2E_r\sqrt{A}}$$

$$\therefore C = C_s + C_f$$

$$C = \frac{\sqrt{\pi}}{2E_r\sqrt{A}} + C_f \tag{17}$$

By invoking the additional assumption explicitly stated earlier surrounding E's insensitivity to depth, one may proportionally reformulate Eq. (17) as follows Eq. (18):

$$C = C_s + C_f$$

$$= \frac{\sqrt{\pi}}{2E_r\sqrt{A}} + C_f$$

$$\therefore C = \frac{\sqrt{\pi}}{2E_r\sqrt{A}} + C_f$$

$$C = \frac{\sqrt{\pi}}{2E_r}\frac{1}{\sqrt{A}} + C_f$$

$$= x\frac{1}{\sqrt{A}} + C_f$$

$$= \frac{x}{\sqrt{A}} + C_f$$

$$C \propto \left(\sqrt{A}\right)^{-1} + C_f$$

$$\therefore C \propto \frac{1}{\sqrt{A}} + C_f \tag{18}$$

As a result, empirically fitting C as a function of $A^{-0.5}$ to a linear expression yields an intercept equal to the load frame compliance contribution. After that, proportional relations may once again be revisited, alongside aforementioned equivalence relations, such that Eq. (18) yields Eq. (19), such that

$$C \propto \frac{1}{\sqrt{A}} + C_f$$

$$\propto \frac{1}{\sqrt{A}}$$

$$\propto \frac{1}{\sqrt{F(h_c)}}$$

$$\propto \frac{1}{\sqrt{24.5h_c^2}} \tag{19}$$

As such, Eq. (19) captures an idealized Berkovich indenter tip geometry (that is, the widely used, three-sided pyramidal tip geometry) such that the curve-fitting procedure associated with C as a function of $A^{-0.5}$ may be pursued for estimating C_f and E_r given the assumption and use of an idealized and perfect Berkovich indenter tip's contact area function. Since C_f and E_r were assumed to be constant as a function of C_s, n-number of indentation size-specific and geometrically ideal contact area values were calculated by the O&P procedure and are easily calculated by modern systems today, via rearrangement of the already presented equations, as shown below via Eq. (20):

$$C = C_s + C_f$$

$$= \frac{\sqrt{\pi}}{2E_r\sqrt{A}} + C_f$$

$$\rightarrow (C - C_f) = \frac{\sqrt{\pi}}{2E_r\sqrt{A}}$$

$$\rightarrow \sqrt{A}(C - C_f) = \frac{\sqrt{\pi}}{2E_r}$$

$$\therefore \sqrt{A} = \frac{\sqrt{\pi}}{2E_r}(C - C_f)^{-1}$$

$$\rightarrow \sqrt{A} = \frac{\sqrt{\pi}}{2E_r(C - C_f)}$$

$$\therefore \left(\sqrt{A} = \frac{\sqrt{\pi}}{2E_r(C - C_f)}\right)^2$$

$$\rightarrow A = \frac{\pi}{4E_r^2(C - C_f)^2}$$

$$\therefore C \propto \frac{1}{\sqrt{A}} + C_f$$
$$\Rightarrow A = F(h_c)$$
$$= x^2(C - C_f)^{-2}$$
$$\rightarrow F(h_c) = x^2 \frac{1}{(C_s(h_c))^2}$$
$$= \frac{\pi}{4E_r^2(C_s(h_c))^2} \tag{20}$$

Accordingly, when the proportionality just presented between the total compliance, as a function of indentation contact depth, and the contact area function as a function of indentation contact, is coupled with surrogate specimen data as well as analytical fitting procedures for the estimation of a calibrated contact area function, machine, tip, and reference specimen dependent calibrations may be pursued on an as-needed basis by a given researcher. In any case, the contact area function analytical fitting procedure may be conceptualized as an up to eight-parameter harmonic average of polynomials, which is expressed as Eq. (21), such that

$$F(h_c) = (24.5)h_c^2 + C_1 h_c + C_2 h_c^{\frac{1}{2}} + C_3 h_c^{\frac{1}{4}} + \cdots + C_8 h_c^{\frac{1}{128}} \tag{21}$$

More to the point, the eight-parameter harmonic average of polynomials given and expressed above takes the mathematical form of a series expression that can be given as Eq. (22) as follows:

$$F(h_c) = \sum_{n=0}^{8} C_n (h_c)^{2-n} \tag{22}$$

The mathematical formulations pursued herein comprise the various aspects of the 1992 method presented by O&P, since $A = F(h_c)$ enables mechanical properties of materials, i.e., E and H, to be assessed at nanomechanical and micromechanical length scales without the need for microscopy-based evaluation of contact areas on a per measurement basis.

Also, worth consideration herein is the appendix to O&P's 1992 manuscript, which was titled Continuous Measurement of Contact Stiffness by a Dynamic Technique. Though dynamic/CSM nanoindentation has emerged as a valuable tool throughout the modern instrumented indentation and nanoindentation community [8], the limited realization of O&P's CSM technique, relative to the time of original publication, reveals scattered attempts by contemporaries in the mid-to-late 1990s to wrestle with not only the OP method and associated manuscript but also the intellectual novelty underpinning the appended framework, as well as the mechanical properties that were eventually found to be measurable via the incorporation of the details presented in the 1992 appendix on dynamic nanoindentation too. That said, forthcoming areas of the present chapter provide details surrounding the wide range of mechanical properties that became experimentally probable due to CSM-based nanoindentation methods. In the meantime, the needs addressed by O&P's peer-reviewed research deliverables detailed in their 1992 manuscript were considered next.

3. Needs addressed by the Oliver-Pharr method

As noted by O&P in 1992, the emergence of thin-film technologies as well as technological advancements, which directly followed from functional thin-film

material development and advancements too, ultimately inspired recognition of the fact that sensing load-displacement behavior via indentation enabled thin film mechanical properties and layered material property extraction [1]. Since such a statement from O&P was concerned with need-based sources of inspiration associated with the early 1980s, i.e., a decade or so before the publication of concern, work undertaken before the present 1992 article attempted to address such needs as effectively as possible.

Needs remained through 1992 and were therefore accordingly addressed, in part, by O&P. However, said needs were separable (categorically speaking) into industrial or materials characterization-based needs and pedagogical or methodological needs. Stated otherwise, needs were classifiable by either the application of nanoindentation, such as micron-scale IIT, or the development and research into nanoindentation as a sub-field of explicit study. Of course, it stands to reason that those advancements in our understanding of nanoindentation, without an underpinning industrial driving force, would nevertheless enable further materials development and research to thrive too. However, without industrial interest and backing, it may very well have taken much more time to reach its' industrially minded status and capabilities when viewed through the lens of technology readiness levels.

Still, the work of O&P was further motivated by materials engineering and science needs within the broader governmental, industrial, academic, collaborative, and technological ecosystem. That being said, one point that ought to be emphasized before further consideration of the emergence of OP mode of nanoindentation testing and analysis is the fact that regardless of the applied materials characterization needs (that is, thin films versus nuclear materials, for example), nanoindentation remains sought after to date, since IIT analysis at nanometric length scales enables small-scale mechanical properties to be explored in a systematic and reproducible manner (so long as the OP method is adhered to).

Consequently, one may reason that, as defined in O&P's original research article, nanoindentation was formalized and developed in commercial forms to serve as a foundational linkage between small-scale properties and mesoscale material behavior. Stated another way, nanoindentation and the OP method of load-displacement data analysis served to, at least in part, address the standing need for probing nanomechanical and micromechanical material strength and mechanical properties alike, regardless of a particular material's industrial intricacies. Of course, industrial sectors beyond applied monolithic materials-based component processing and production would ultimately be influenced by nanoindentation testing too. Such influences were found to be true given nanoindentation's widespread and successful adoption by the polymeric [9], biological [10], and composite material sectors, too [11].

In keeping with the passage above, recall once more that O&P attempted to address the need for a small-scale mechanical property evaluation method and an experimental system to do so, which became known as a nanoindenter. As stated by O&P, such an instrument could be classified as a mechanical property's microprobe [1]. Indeed, small-scale capabilities were reportedly achieved by O&P in 1992, wherein the Nano Instruments, Inc., Nanoindenter, which was housed at Oak Ridge National Laboratory (Oak Ridge, TN, USA), achieved a load resolution of 0.3 μN and a displacement resolution of 0.16 nm; in turn, maintaining sub-micrometer and therefore small-scale resolution.

Having presented the mathematical analysis and manipulation underlying O&P's 1992 approach to nanoindentation data analysis, in addition to **Figure 1(b)**'s rendering of a cross-section of an indenter tip loaded upon a hypothetical target material or specimen, note that additional visualizations or schematics are provided

in Ref. [1] too. O&P presented a schematic graphical representation of a load vs. depth nanoindentation curve for further context; a schematic detailing how the Nano Instruments, Inc., Nanoindenter was assembled; and an SEM image or micrograph of nanoindented fused Si specimen after reaching a maximal applied load of 40 mN [1], for instance.

O&P also stated that practical reasons, such as cost and difficulty of resolving micrographs of shallow indents at the time, underpinned the need for calculating the geometry of indentation-induced residual impressions such that contact areas could be determined [1]. Such a statement attests to another need-based thought process by O&P, wherein they document how effectively microscopy-free nanoindentation was able to be procured by O&P in 1992. Reflecting on such a need in 2004, O&P also noted the fact that their 1992 methodology for hardness and modulus determination from load-depth data via ITT inspired techniques had been widely adopted for small-scale mechanical characterization of materials, suggesting that said widespread adoption was largely due to the microscopy-free nature of the OP method [12].

Returning to materialistic needs addressed by O&P, Chen et al. noted that mechanical property determination of thin films was mainly driven by the needs and desires expressed semiconductor and magnetic storage materials engineers [13]. Prior to the work of Chen et al., Menčík et al. noted that a significant mechanical property of interest to the thin film community was the hardness of the thin film and the thin film elastic modulus [14]. The determination of the modulus of elasticity associated with a functional thin film was critical to the evaluation of residual stresses via X-ray based analysis; the deduction of deformation-driven thermomechanical stress accumulation within the thin film as the film-substrate component is subject to an externally applied load; and even the determination of delamination mechanics [14].

Thus, one need not be surprised that even though O&P only made mention of thin-film mechanics in 1992, to identify motivations for nanoindentation research and development, the OP method of analysis emerged as a standard nanoindentation load-displacement data analysis framework that became [15], and remains [16], commonly applied to thin films. Nevertheless, as noted by Saha and Nix a decade after O&P's 1992 article, O&P formulated the OP method using monolithic materials, i.e., non-composite-like components [17]. Regardless, one may still reason that O&P indirectly, although intentionally, laid the experimental groundwork for thin-film mechanical property evaluation via IIT modes of analysis, which has since been refined further following 1992 innumerable works, such as those associated with [18]. Additionally, one may also note the fact that the need for sub-micrometric mechanical characterization also followed from the limitations of the otherwise employed micro-beam bending and film deflection testing methods for thin-film elastic modulus assessment [19], among other approaches, which were identified in 1990 by Alexopoulos et al. [20].

4. State of the art prior to Oliver-Pharr methodology

Before the publication of O&P's 1992 research article, which has since matured into one of the most highly cited and influential manuscripts in the field of materials science and engineering to date, nanoindentation as a commercialized technological advent was developed by John Pethica, Ron Hutchings, and Warren Oliver in 1983 while Pethica, Hutchings and Oliver were working together at Brown Boveri in Switzerland [21]. Accordingly, such a timeline provides a relatively lower bound for prior work considerations in the decade preceding the 1992 publication alongside

the understanding of nanoindentation garnered after Pethica et al. initiated their collaboration in the 1980s [22]. Hence, the present chapter refocuses upon the state of the art between the innovative development of a nanoindenter/IIT in the early 1980s and O&P's 1992 article. The remaining portion of the present section is dedicated to nanoindentation or IIT developments between 1982 and 1992.

In so far as work related to the state-of-the-art surrounding indentation analysis before OP methodological formalization, prior work may be initiated herein via considering the work of Newey et al., which was published in 1982 [23]. Specifically, Newey et al. documented an ultra-low-load penetration hardness tester and testing approach that also employed a non-optical method of residual indent geometry deduction while continuously recording indenter tip penetration depths well as applied loads too. Remarkably, Newey et al.'s ultramicrohardness tester achieved a load resolution of 10 μN, a depth resolution of approximately 5 nm, and a maximal load of 3 mN. Moreover, unlike Newey et al.'s counterparts, such as Nishibori et al. in Refs. [24–26], or Frohlich et al. [27], Newey et al.'s approach resulted in indenter probe penetration depth recording as a function of the load applied and the time required to reach said load, therefore enabling time- and load-dependent indentation-induced mechanisms to be observed.

At the same time, Newey et al.'s ultra-low-load penetration hardness tester was able to capture an indicator of material elasticity and even adhesion properties via testing too. Thus, like O&P's objectives surrounding the development of an understanding as to how to formulate more wear-resistant metallic surfaces via ion implantation for tribological enhancement [21], Newey et al.'s advancements were to investigate hardness as a function of ion-based implantation processing of materials.

Newey et al.'s approach agreed with the precedent established by E. S. Berkovich surrounding the suitability of three-sided pyramidal tip geometries over that of Knoop and Vickers tip geometries because of the inherent fact that Berkovich tips (i.e., a particular form of three-sided pyramidal tips) meet at only one apex point. Moreover, Newey et al. invoked the proportionality shared between pyramidal indentation depth and applied load when an (assumed) ideal plastic material was undergoing indentation testing, such that the following theoretical relation (Eq. (23)) between hardness (H_v), force (F), and depth (δ), in base units, was turned to, such that

$$H_v = \frac{0.0378(F)}{\delta^2} \tag{23}$$

Later, Eq. (23) was amended to include on-load and off-load hardness analysis by way of including elastic and plastic indentation contributions via the use of $\delta_T - \delta_e$ in place of δ; thus, overcoming the assumption of an idealized, fully plastic material, which had been reflected in Eq. (23). In all, Newey et al. noted that the off-load depth of $\delta_T - \delta_e$ maintained a 5–10% difference with an independently assessed depth, denoted as δ_A, and obtained via ex-situ microscopy analysis post-indentation. However, one must note that the work of Newey et al. was limited to indium (primarily) and electropolished AISI 52100 steel and rock salt, thus prohibiting the 5–10% difference acquired be fully generalize-able across metallic, ceramic, composite materials too.

Moreover, the 5–10% difference between $\delta_T - \delta_e$ in contrast with δ_A, when substituted into Eq. (23) in place of δ, resulted in an overestimation of the hardness by 10–20% when their non-microscopy or microscopy-free depth determination method was invoked. Still, Newey et al. quickly addressed such a discrepancy between their microscopy-free depth determination and microscopy-based

counterbalance through the lens of pile-up effects; therefore, suggesting that the 10–20% difference in H_v (i.e., the Vickers hardness number or value) as a function of δ was an artifact of overestimated microscopy-based depths. Finally, Newey et al. correctly pointed out that a phenomenon concerning the non-transferable nature of hardness values obtained using their ultra-microhardness tester, in contrast with a Vickers or Knoop indenter, could be explained through the lens of mean contact pressure or indentation hardness value depth dependence. In doing so, Newey et al. stumbled upon what would later be articulated as an indentation size effect (ISE) that came to be described through the lens of strain gradient plasticity and ultimately unveiled subsequent work by Nix and Gao [28].

Shortly after Newey et al.'s 1982 article, Pethicai et al. highlighted an indentation advancement in a 1983 article focused upon the realm of hardness testing at depths as low as 20 nm [22]. In doing so, Pethicai et al. utilized Ni, Au, and Si to demonstrate that indentation contact areas determined via post-indentation electron microscopy were quantifiable when coupled with the 1908-rooted mathematical formulation of Meyer's hardness. Interestingly, just as Newey et al. noted an ISE prior to Nix and Gao's strain gradient plasticity framework, Pethicai et al. also noted an increase of IIT hardness as a function of smaller indentation size at the submicron length scale [22]. In addition, Pethicai et al. observed relatively increased hardness values at shallow indentation depths and relatively decreased hardness values at greater indentation depths. Finally, like the ultramicrohardness tester developed by Newey et al., indentation load-depth relations were also continuously recorded by Pethicai et al. via loading and unloading cycles such that a quantitative understanding of elastic relaxation could be formulated.

Building upon Pethicai et al.'s novel advancement of indentation abilities into the nm depth regime, Oliver published a subsequent article in 1986, which noted that the technological groundwork, hardware, and understanding of the indentation process had been under development [29]. Said statement by Oliver highlights the pre-1992 state of the art surrounding small volume mechanical property inspection by the mid-1980s. The limited degree of understanding within the respective research community highlights the significant gap addressed by O&P in their 1992 manuscript. Oliver noted that indent geometry determination was not only particularly difficult through microscopy but was also connected to the most critical parameter in relation to contact area determination relative to the specimen and indenter tip. Oliver went so far as to state that a mechanical properties microprobe was not only conceptually exciting but was also being complemented by concomitant advancements in understanding and hardware needed to actualize a submicron resolution system for recording mechanical response and behavior during indentation. Such an assertion readily situates the implications of Oliver's ongoing efforts at the time.

In keeping with the trend of developing practical submicron indentation testing, Doerner et al. considered thin-film plasticity properties compared to substrate curvature techniques [30]. Around the time that Doerner et al. published their submicron indentation testing of thin films and respective findings, Doerner et al. also proposed a nanoindentation data analysis and interpretation framework that was purportedly based upon the use of the commercial nanoindentation system from Nano Instruments, Inc. [2]. Continuation along similar lines to the work detailed in Ref. [30] was also pursued by Oliver et al. in 1987 [31]. During that very same year, the interactive forces associated with a microprobe or nanoprobe indenter tip and a target specimen with a flat surface, as well as the tip-specimen surface responses, were documented in Ref. [32]. Consequently, Pethica and Oliver demonstrated that a true contact area was discernible when local surface stiffness values were measured via the application of an alternating current force to the

indenter tip. Said findings were explored beyond nanoindentation and the concurrent emergence of atomic force microscopes and scanning tunneling microscopy enclosed tips.

Consideration of state of the art, pre-1992, must also include the eventual patent and patent-related documentation associated with the commercialization of the Nanoindenter by Pethica and Oliver as of 1989, which was entitled as follows in Ref. [33]: A Method for Continuous Determination of the Elastic Stiffness of Contact Between two Bodies. Beyond the description afforded from the title provided, Pethica and Oliver stated that an ultra-low load IIT/nanoindentation system known as the Nanoindenter and commercially available through Microsciences, Inc. (Norwell, MA, USA) was substantially modified as part of the invention detailed as part of the patent. Said modification to the Nanoindenter allowed the force to be linearly modulated (increased or decreased) via electromotive means throughout various loading rates. The further modification enabled a capacitive displacement gage to be used to determine the indentation area as a function of indenter displacement following initial contact between a target specimen surface and an indenter probe. With said modifications in mind and others detailed directly within the patent under consideration, Pethica and Oliver ultimately devised a means of continuously determining the elastic contact stiffness between two bodies.

Around the point in time that the patent was assigned to the inventors and the U.S. Department of Energy, the materials science and engineering research community poised to benefit from nanoindentation centered characterization capabilities began applying initial approaches to load-displacement data analysis, which concomitantly started to emerge alongside the protocols laid out by O&P in the early 1990s. Furthermore, said research community started coupling the utilization of preliminary, or initialized, approaches to load-displacement data analysis with early versions of the commercially available Nanoindenter and low-load indenters generally; ultimately, applying them to various material systems. For example, Stone et al. published findings surrounding their application of such a mechanical properties microprobe as detailed in Ref. [34]. Specifically, Stone et al. applied continuous indentation testing to sputter-deposited Al thin films adhered to Si substrates.

In addition to the work of Stone et al., Loubet et al. built their micro-indenter-that could record load-depth curves, including both loading and unloading load-displacement curves, to explore the complex phenomena underlying MgO Vickers indentation data in Ref. [35]. Another example was detailed in Ref. [36], wherein Pharr and Oliver applied the state-of-the-art understanding and their own methodological improvements to IIT data analysis and testing pre-1992 to directly link hardness as a function of depth with dislocation structures in a single crystal Ag specimen. Such exploration was performed to contextualize better deformation mechanisms, elasto-plasticity, and plasticity in a pure metal specimen.

Ultimately, during the final years preceding the publication of O&P's paper in 1992, state of the art surrounding small-scale IIT was primarily found to be concerned with refining and proposing physical, computational, foundational, empirical, numerical, and/or theoretical relationships to yield a mechanistic abstraction for experimentally consistent models, which could be used in IIT data analysis. Nevertheless, the clear need for the OP nanoindentation testing methodology and load-depth data analysis protocol can be adequately appreciated through the simple fact that their novel approach avoided any superfluous explanations and instead focused on analytical patterns that could be discerned and replicated by others time and again, as will be discussed in Part 2.

5. Developments immediately following Oliver-Pharr's method

Between 1992 and 2002, there were numerable application-specific and application-inspired uses of nanoindentation and OP-based method and analysis use cases that could have been widely considered herein [37]. However, in so far as the post-OP publication state-of-the-art may be considered, one ought to note that enumerable investigations went on to critically examine the 1992 article by O&P and the OP testing and analysis method or framework. In conjunction with others during the respective period, some critical examinations formulated novel physical and mechanical relationships to extend the range of possibilities associated with sub-micron indentation deformation.

Therefore, one may begin the consideration of the respective decade following O&P's 1992 article by invoking the 1993 article, entitled Mechanical Characterization Using Indentation Experiments, by Oliver et al. [38]. Remarkably, by 1993, Oliver et al. noted that nanoindentation-based methods for assessing the creep stress exponent were formulated; therefore, clearly highlighting a successful extension of small volume indentation testing and analysis for mechanical properties assessment purposes that went beyond hardness and modulus alone just one year after the 1992 paper was published. Moreover, Oliver et al. also noted that additional improvements were also presented and went beyond the improved techniques prescribed by O&P just one year prior.

As time and attention progressed and evolved within the indentation-based research and development community, critical takes concerned with the OP data analysis and testing technique emerged as early as 1996 (if not earlier). Stated otherwise, a subset of the mechanical-properties-minded materials science and engineering world began to present alternative load-depth analysis procedures that were free of assumptions surrounding elastic material compatibility with depth-sensing indentation and even the OP approach in general. Other alternatives also noted concerns surrounding the reliance of OP upon a mean contact pressure definition of hardness, rather than that of energy-related principles (like that of the work of indentation), and even alongside a Meyers hardness perspective.

One of the early papers presenting such an alternative IIT load-displacement data analysis approach was rooted in the mechanical work of indentation, which may be thought of as a physical rendering of force and displacement at its' core and published in the mid-1990s by Gubicza et al. [39]. Beyond consideration of theory alone, Gubicza et al. also indirectly suggested that O&P's approach still performed just as well in achieving mechanical property evaluation compared with Gubicza et al.'s novel and semi-empirical depth-sensing indentation data analysis approach. Furthermore, Gubicza et al. stated that the hardness deduced agreed well with the OP method for many materials [39].

Still, Gubicza et al.'s critical take on the work of O&P was well-substantiated in so far as, ideally, elastic materials were of interest, for instance. However, in so far as the veracity of the work of Gubicza et al. is concerned, one ought to note that Gubicza et al.'s measurements and criticisms were levied using applied indentation pressures as high as 100 N, which resides within the macro-hardness regime rather than the micro-hardness and nano-hardness regimes initially affiliated with the OP technique as of 1992. Furthermore, the criticisms and critical takes levied by Gubicza et al., in so far as their findings were related and comparable to the findings of O&P, must be met with additional skepticism since they used a computer-controlled, Vickers indenter equipped, and hydraulic, mechanical testing device to perform depth-sensing indentation for hardness evaluation. Gubicza et al.'s elected use of such an IIT or indentation set-up and system controlled hydraulically rather

than electromagnetically (in the case of the OP framework) prohibits genuine comparative analysis when considering the varied tip geometry, loading and depth recording sensitivities, and the like.

Beyond the initial considerations just detailed and discussed, a genuine pillar of the post-1992 OP-influenced era follows from the work of Field and Swain that was published in 1995. Indeed, Field and Swain's work has continued to garner traction through the present day because of Field and Swain's suspicion that sub-micrometer spherical and cyclic (i.e., partial loading-and-unloading cycles during a global loading-and-unloading process) nanoindentation testing could be used and extended into the realm of capturing mechanical flow curves and stress vs. strain plasticity phenomena. Such a window into mechanical flow behavior via Field and Swain's approach, or any other respectively similar approach concerned with indentation as the means of flow curve calculation, becomes particularly important when volumes of material in need of mechanical characterization cannot be characterized via traditional uniaxial tension or compression methods due to inherent size limitations. Accordingly, Field and Swain stated that spherical tip-based sub-micron indentation testing potentially housed the key to determining hardness, elastic modulus, representative stress vs. strain or mechanical flow curves, and strain hardening behaviors for size-limited material volumes [40].

As such, Field and Swain's representative spherical indentation stress vs. strain plot for a steel specimen, the physical condition of cono-spherical tips employed, and the degree of pile-up observed in one of the materials Field and Swain considered in their work. Advents since the time of Field and Swain rendered concerns surrounding the integrity of their approach since the size of the indents considered by Field and Swain suggests that Field and Swain surpassed the transitional limit of the spherical apex of their tips, which indicates that they unknowingly reported conical, rather than spherical, representative stress vs. strain curves at quite large indentation strains. In modern times, authors such as Sousa et al. in Refs. [41–43] and Leitner et al. in Refs. [44, 45] have consistently warned of the consequences surrounding the use of cono-spherical tips beyond their sphere-to-cone transition point, which results in a violation of Hertzian contact mechanics and geometrically defined stress-strain evolution.

Apart from the work of Field and Swain, the present section will also entertain further progress reportedly made pre-2002. In turn, attention is refocused upon another matter of depth-sensing indentation measurement that influences recorded load-displacement data and subsequently derived mechanical properties. Of particular focus at the respective point in time continued to consider the influences of pile-up and sink-in came into focus as findings suggested that improper accounting of pile-up can lead to the overestimation of hardness (since the area term associated with the denominator of Eq. (9) would be smaller than that corrected for pile-up, for example). Hence, Bolshakov and Pharr explored such matters in Ref. [46].

During the work by Bolshakov and Pharr, finite element analysis (FEA) of conical indentation of a variety of elastic-plastic materials were analyzed in-silico, enabling Bolshakov and Pharr to discover that underestimation of load-displacement curve derived contact areas could reach up to 60% when indentation-induced pile-up is large relative to indentation depth. Ultimately, Bolshakov and Pharr identified the ratio between h_f and h_{max} measured parameters associated with recorded load-displacement data. One may take note of specimens wherein pile-up deserves more significant consideration than that of a correction factor, for example. Such a parameter was expressed as h_f/h_{max}, wherein a ratio less than or equal to 0.7 indicates that a material is not likely to be significantly affected by pile-up such that reasonable results are procurable via OP data analysis. Of course, the opposite was true when $h_f/h_{max} > 0.7$

6. Conclusion

The present chapter described the emergence of nanoindentation testing and analysis within the materials science and engineering literature. Emphasis was placed upon the origins of the dominant mode of submicron instrumented indentation testing and analysis (known as the Oliver-Pharr method). Specifically, detailed reconsideration and formulation of the Oliver-Pharr method was provided, followed by the industrial, engineering, manufacturing, and materials engineering R&D needs that were able to be addressed through the application of the Oliver-Pharr method. In detailing the emergence of Oliver and Pharr's approach to nanoindentation data analysis, the state of the art between the development of a nanoindenter in the early 1980s and formal publication of the Oliver-Pharr method in 1992 was presented. Next, several noteworthy and documented nanoindentation developments post-1992 were considered and contextualized. Continued consideration of the subsequent advancements, discoveries, innovations and attempts to realize nanoindentation's potential as an instrumented strength microprobe are described next in Part 2.

Author details

Bryer C. Sousa[1]*, Jennifer Hay[2] and Danielle L. Cote[1]

1 Department of Mechanical and Materials Engineering, Worcester Polytechnic Institute, Worcester, MA, USA

2 KLA Instruments (Oak Ridge, TN), KLA, Milpitas, CA, USA

*Address all correspondence to: bcsousa@wpi.edu

IntechOpen

References

[1] Oliver WC, Pharr GM. An improved technique for determining hardness and elastic modulus using load and displacement sensing indentation experiments. Journal of Materials Research. 1992;**7**(6):1564-1583

[2] Doerner MF, Nix WD. A method for interpreting the data from depth-sensing indentation instruments. Journal of Materials Research. 1986;**1**(4):601-609

[3] Alisafaei F, Han CS. Indentation depth dependent mechanical behavior in polymers. Moshchalkov VV, editor. Adv Condens Matter Phys. 2015;**2015**: 391579

[4] Bulychev SI, Alekhin VP, Shorshorov MK, Ternovskij AP, Shnyrev GD. Determination of Young modulus by the hardness indentation diagram. Zavodskaya Laboratoria. 1975; **41**(9):1137-1140

[5] Poon B, Rittel D, Ravichandran G. An analysis of nanoindentation in linearly elastic solids. International Journal of Solids and Structures. 2008;**45**(24): 6018-6033

[6] Sneddon IN. The relation between load and penetration in the axisymmetric boussinesq problem for a punch of arbitrary profile. International Journal of Engineering Science. 1965; **3**(1):47-57

[7] Chandler H. Hardness Testing. 2nd ed. Materials Park, OH: ASM International; 1999. p. 210

[8] Fischer-Cripps AC. Multiple-frequency dynamic nanoindentation testing. Journal of Materials Research. 2004;**19**(10):2981-2988

[9] Tranchida D, Piccarolo S, Loos J, Alexeev A. Mechanical characterization of polymers on a nanometer scale through nanoindentation. A study on pile-up and viscoelasticity. Macromolecules. 2007;**40**(4):1259-1267

[10] Ebenstein DM, Pruitt LA. Nanoindentation of biological materials. Nano Today. 2006;**1**(3):26-33

[11] Hu C, Li Z. A review on the mechanical properties of cement-based materials measured by nanoindentation. Construction and Building Materials. 2015;**90**:80-90

[12] Oliver WC, Pharr GM. Measurement of hardness and elastic modulus by instrumented indentation: Advances in understanding and refinements to methodology. Journal of Materials Research. 2004;**19**(1):3

[13] Chen S, Liu L, Wang T. Investigation of the mechanical properties of thin films by nanoindentation, considering the effects of thickness and different coating–substrate combinations. Surface and Coating Technology. 2005;**191**(1):25-32

[14] Menčík J, Munz D, Quandt E, Weppelmann ER, Swain MV. Determination of elastic modulus of thin layers using nanoindentation. Journal of Materials Research. 1997;**12**(9): 2475-2484

[15] Hay J, Crawford B. Measuring substrate-independent modulus of thin films. Journal of Materials Research. 2011;**26**(6):727-738

[16] Li H, Chen J, Chen Q, Liu M. Determining the constitutive behavior of nonlinear visco-elastic-plastic PMMA thin films using nanoindentation and finite element simulation. Materials and Design. 2021;**197**:109239. ISSN: 0264-1275

[17] Saha R, Nix WD. Effects of the substrate on the determination of thin

film mechanical properties by nanoindentation. Acta Materialia. 2002; **50**(1):23-38

[18] Alaboodi AS, Hussain Z. Finite element modeling of nano-indentation technique to characterize thin film coatings. J King Saud Univ - Eng Sci. 2019;**31**(1):61-69

[19] Nix WD. Mechanical properties of thin films. Metallurgical Transactions A. 1989;**20**(11):2217

[20] Alexopoulos PS, O'Sullivan TC. Mechanical properties of thin films. Annual Review of Materials Science. 1990;**20**(1):391-420

[21] Oliver WC, Pharr GM. Nanoindentation in materials research: Past, present, and future. MRS Bulletin. 2010;**35**(11):897-907

[22] Pethicai JB, Hutchings R, Oliver WC. Hardness measurement at penetration depths as small as 20 nm. Philosophical Magazine A. 1983;**48**(4): 593-606

[23] Newey D, Wilkins MA, Pollock HM. An ultra-low-load penetration hardness tester. J Phys [E]. 1982;**15**(1):119-122

[24] Nishibori M, Kinosita K. Ultra-microhardness of vacuum-deposited films I: Ultra-microhardness tester. Thin Solid Films. 1978;**48**(3):325-331

[25] Tazaki M, Nishibori M, Kinosita K. Ultra-microhardness of vacuum-deposited films II: Results for silver, gold, copper, MgF2. LiF and ZnS. Thin Solid Films. 1978;**51**(1):13-21

[26] Nishibori M, Kinosita K. Ultra-microhardness of some vacuum-deposited films. Japanese Journal of Applied Physics. 1974;**13**(S1): A862B

[27] Fröhlich F, Grau P, Grellmann W. Performance and analysis of recording microhardness tests. Physica Status Solidi A: Applications and Materials Science. 1977;**42**(1):79-89

[28] Nix WD, Gao H. Indentation size effects in crystalline materials: A law for strain gradient plasticity. Journal of the Mechanics and Physics of Solids. 1998; **46**(3):411-425

[29] Oliver WC. Progress in the development of a mechanical properties microprobe*. MRS Bulletin. 1986;**11**(5): 15-21

[30] Doerner MF, Gardner DS, Nix WD. Plastic properties of thin films on substrates as measured by submicron indentation hardness and substrate curvature techniques. Journal of Materials Research. 1986;**1**(6):845-851

[31] Oliver WC, McHargue CJ, Zinkle SJ. Thin Film Characterization Using a Mechanical Properties Microprobe [Internet]. TN, USA: Oak Ridge National Lab.; 1987. Report No.: CONF-870388-5. Available from: https://www.osti.gov/bib lio/6643878-thin-film-characterization-using-mechanical-properties-microprobe [Cited: 23 November 2021]

[32] Pethica JB, Oliver WC. Tip surface interactions in STM and AFM. Physica Scripta. 1987;**T19A**:61-66

[33] Oliver WC, Pethica JB. Method for continuous determination of the elastic stiffness of contact between two bodies [Internet]. US4848141A; 1989. Available from: https://patents.google.c om/patent/US4848141A/en [Cited: 23 November 2021]

[34] Stone D, LaFontaine W, Alexopoulos P, Wu T, Li C. An investigation of hardness and adhesion of sputter-deposited aluminum on silicon by utilizing a continuous indentation test. Journal of Materials Research. 1988;**3**:141-147

[35] Loubet J, Georges J, Marchesini O, Meille G. Vickers indentation curves of

magnesium oxide (MgO). J Tribol-Trans Asme. 1984;**106**:43-48

[36] Pharr G, Oliver W. Nanoindentation of silver-relations between hardness and dislocation structure. Journal of Materials Research. 1989;**4**:94-101

[37] Pharr GM, Oliver WC. Measurement of thin film mechanical properties using nanoindentation. MRS Bulletin. 1992;**17**(7):28-33

[38] Oliver WC, Lucas BN, Pharr GM. Mechanical characterization using indentation experiments. In: Nastasi M, Parkin DM, Gleiter H, editors. Mechanical Properties and Deformation Behavior of Materials Having Ultra-Fine Microstructures. Dordrecht: Springer Netherlands; 1993. pp. 417-428

[39] Gubicza J, Juhász A, Lendvai J. A new method for hardness determination from depth sensing indentation tests. Journal of Materials Research. 1996;**11**(12):2964-2967

[40] Field JS, Swain MV. Determining the mechanical properties of small volumes of material from submicrometer spherical indentations. Journal of Materials Research. 1995;**10**(1):101-112

[41] Sousa BC, Sundberg KL, Gleason MA, Cote DL. Understanding the antipathogenic performance of nanostructured and conventional copper cold spray material consolidations and coated surfaces. Crystals. 2020;**10**(6): 504

[42] Sousa BC, Gleason MA, Haddad B, Champagne VK, Nardi AT, Cote DL. Nanomechanical characterization for cold spray: From feedstock to consolidated material properties. Metals. 2020;**10**(9). Available from: https://www.mdpi.com/2075-4701/10/9/1195

[43] Sundberg K, Sousa BC, Schreiber J, Walde CE, Eden TJ, Sisson RD, et al. Finite element modeling of single-particle impacts for the optimization of antimicrobial copper cold spray coatings. Journal of Thermal Spray Technology. 2020;**29**(8):1847-1862

[44] Leitner A. Advanced Nanoindentation Techniques for the Extraction of Material Flow Curves. University of Leoben. 2018

[45] Leitner A, Maier-Kiener V, Kiener D. Essential refinements of spherical nanoindentation protocols for the reliable determination of mechanical flow curves. Materials and Design. 2018; **146**:69-80

[46] Bolshakov A, Pharr GM. Influences of pileup on the measurement of mechanical properties by load and depth sensing indentation techniques. Journal of Materials Research. 1998;**13**(4): 1049-1058